Petroleum Research 9 (2024) 61–71

Contents lists available at ScienceDirect

Petroleum Research

journal homepage: http://www.keaipublishing.com/en/journals/petroleum-research/

Full Length Article

High resolution sequence stratigraphy of the Mishrif Formation (Cenomanian-Early Turonian) at zubair oilfield (al-rafdhiah dome), southern Iraq

Aymen A. Lazim [a], Maher J. Ismail [b], Maher M. Mahdi [c, *]

[a] Geoscience Department, Zubair Field Operation Division, Basra Oil Company, Iraq
[b] Basrah Oil Company, WQ1 FOD, Basrah, Iraq
[c] University of Basrah, College of Science, Geology Dept., Basrah, Iraq

ARTICLE INFO

Article history:
Received 16 September 2022
Received in revised form
28 July 2023
Accepted 7 August 2023
Available online 8 August 2023

Keywords:
Mishrif formation
Cenomanian
Sequence stratigraphy
Zubair oilfield
Iraq

ABSTRACT

The Mishrif Formation (Cenomanian -E Turonian) is one of the most important geological formations in the Middle East and Iraq because it contains enormous petroleum accumulations. It is considered to be the first reservoir in the region, and is still being studied because of its economic significance. The carbonate of the Mishrif Formation derives from a variety of depositional settings, including mid-ramp, shoal, lagoon, and intertidal. The five main microfacies discussed in this paper are wackestone, packstone, grainstone, floatstone, and bindstone. The most frequent fossilised components found in the Mishrif Formation are rudists, benthic foraminifera, echinoderms, burrows molluscs, and algae. According to the microfacies and analysed wireline log data, the sequence stratigraphy of the studied formation is composed of two regression cycles. Five parasequences of transgressive–regressive cycles make up the depositional sequence of the Mishrif Formation. The standard depositional environments seem to demonstrate a gradual regression, beginning with a short period of the outer ramp, then a steady period of the mid-ramp, and ending in the intertidal environment. Additionally, the study recorded two regional maximum flooding surfaces: K-135 and K-140. The former is present in the lowermost part of the formation, while the other lies in the middle. This study shows a close relationship between facies (environments) and hydrocarbon accumulation. The increased accumulation focuses on the lower part of the studied formation, and seems to be lower in the upper part of the formation as a result of changes in the environment of deposition.

1. Introduction

The major hydrocarbon system in the Mesopotamian basin dates back to the early Cretaceous–Miocene eras. This petroleum system consists of petroleum source rocks (Sulaiy and Yamama formations), cap rocks (Tanuma, Shiranish, and Rus formations), and reservoir rocks (Tanuma, Yamama, Zubair, Nahr Umr, and Mishrif formations) (Aqrawi et al., 2010; Handhal and Mahdi, 2016). Cretaceous carbonates are distinctive in the Middle East stratigraphic column because a vast amount of hydrocarbon-bearing reservoir units have been found. For the Mesozoic and Cenozoic eras, the Middle East was broadly divided into three primary basins: the East Mediterranean, the Mesopotamian, and the Rub-AlKhali; these were divided by the Hail and Hadheramaut arches (Al-Sherwani, 1983). According to Buday and Jassim (1987) and Jassim and Goff (2006), Iraq can be divided into three tectonic zones: Zagros folded zone, the stable shelf, and the Mesopotamian zone. The current study area is in the Zubair subzone of the Mesopotamian zone, which also includes the Euphrates and Tigris subzones. The most recent tectonic division of Iraq, presented by Fouad (2015), places the study region in Mesopotamia's Outer Platform. The foredeep is the main section of the Zagros foreland basin, which is essentially a flat terrane covered by Miocene–Holocene marine and continental deposits. The objective of this research is to develop a facies analysis architecture that considers microfacies and environmental settings; this will be a useful tool in carbonate reservoir stratigraphy.

* Corresponding author. Correspnding author.
E-mail address: maher.mahdi@uobasrah.edu.iq (M.M. Mahdi).

https://doi.org/10.1016/j.ptlrs.2023.08.002

The studied formation is the most vital carbonate reservoir in Iraq, containing approximately 30% of Iraqi oil reserves (Aqrawi et al., 2010). The period of the Mishrif Formation was the middle Cenomanian–early Turonian age, when thick carbonates were collected and deposited on a basin-wide shallow-water platform (Chatton and Hart, 1961). The Mishrif Formation was defined by Rabanit (1952) at Well Zb-3, and represents the type of section in Iraq. The Mishrif Formation signifies the upper part of the high-stand of the Wasia Group of AP8. The lithology of the Mishrif Formation is composed of different types, including bioclastic, rudist, grey-white limestone, and foraminiferal-rich facies capped by limonitic limestone (Jassim and Goff, 2006). The environments of the Mishrif Formation gradually shift from mid-ramp to lagoonal supratidal environments (Sharland et al., 2001; Al-Ali et al., 2019). According to the carbonate ramp system, shallow water is cyclically prepared for the deposition of the Mishrif carbonate deposits. The Mishrif Formation is classified as part of the AP8 mega sequence, fourth super sequence, and upper part of the Wasia group. The Mishrif Formation is overlapped by the Khasib Formation, which features a clear contact that represents an early-to mid-Turonian unconformity. The lower contact of the conformity surface is with the Rumaila Formation (Sharland et al., 2001; Almohsen, 2019). Because the Mishrif Formation is a giant oil reservoir, it is heavily studied. The addition of new information about the formation from each new study contributes to the knowledge of its history and the environment surrounding the formation. The most important of these studies are carried out by Owen and Nasr (1958), Al-Khersan (1975), Al-Sherwani (1983), Aqrawi et al. (1998), Razoian (2002), Handhel (2006), Aqrawi and Horbury (2008), Al-Rubiay (2009), Al-Maliki (2009), Al-Dulaimy (2010), Al-Najm (2013), Mahdi et al. (2013), Mahdi and Aqrawi (2014), Awadeesian et al. (2015), Al-Ali et al. (2019), Almohsen (2019), Zhao et al. (2019), and Ismail et al. (2021).

In northern Iraq, the Mishrif Formation is equivalent to the Gir-Bir Formation and Dokan formations, which were deposited in the deeper eastern and interbasinal parts of the same basin. Regionally, it is equivalent to the Wasia Group in Saudi Arabia (Cenomanian age) because of the same fossils of foraminifera, rudist, and algae (Al-Sherwani, 1983). In south-eastern Iran, the same fossils have been documented in the upper part of the Sarvak Formation (Al-Sharhan and Nairn, 1988). The Mishrif Formation is equivalent to the Magawa Formation in Kuwait (Powers, 1962) and the Natih Formation in Oman (Member E) (Scott, 1990), as well as to the important Salabikh Formation in the United Arab Emirates (Al-Najm, 2013). The formation has the same name (Mishrif) in Qatar and Bahrain (Handhel, 2006), and is equivalent to the Judea Formation in central and northeast Syria and the Mardin Formation in southeast Turkey (Jassim and Goff, 2006). The Mishrif Formation is widely considered the second most prolific oil reservoir in southern Iraq (Al-Sherwani, 1988), and most of the mentioned regional formations are also producing oil; therefore, this formation is considered one of the most important formations in geological history. This study addresses the relationship between the sedimentology of the Mishrif Formation and the sequence stratigraphy in the Zubair oilfield in southern Iraq at the Al-Rafdhiah dome, describing the details of the sedimentological setting during the deposition of the Mishrif Formation. Transgression and regression events are correlated between this study and the previous studies. This study aims to divide the formation into fourth-order sequence stratigraphic sequences in the Zubair oilfield by using thin sections and wireline log data. This is important because no current detailed study in this field mentions the most imperative microfacies and the diagenesis processes, or the relationship between sequence stratigraphy and hydrocarbon accumulation.

2. Geological setting

The Basrah Petroleum Company discovered the Zubair oil field in 1949. It has 4.5 billion barrels of oil, and production presently exceeds 490,000 barrels per day. According to the field's expansion plan, production will reach a peak of 1.125 million barrels per day in the upcoming years (Almalikee and Souvik, 2021). The Zubair oilfield lies 20 km to the west of Basrah city in southern Iraq, and in the north is bordered by the northern plunge of the Nahr Umr oilfield, to the west by Rumaila, and the southwest by Kuwait (Fig. 1) (Mahdi et al., 2021a; Al-Kaabi et al., 2023).

Al-Hummar and Al-Rafdhiah are two domes in the Zubair oilfield. A saddle separates the two domes, and the Hummar basement fault may have an impact on the area (Al-Mutury and Al-Asadi, 2008). Other studies have divided the field into four domes: Safwan, Al-Rafdhyia, Shuaiba, and Hammar (Al-Jafar and Al-Jaberi, 2019). The oilfield is 67 km long and 8.7 km wide (Al-Mutury and Al-Mayahi, 2010), and there is an average difference of 110 m between the two domes (Al-Hummar and Al-Rafdhiah) (Al-Kaabi et al., 2023).

The petroleum system data indicate that the origin of the oil in the Mishrif Formation is from the Najma/Sargelu formations at Upper Jurassic age, or the Sulaiy and Yamama formations during the Lower Cretaceous age (Al-Ameri et al., 2009). According to the results of this investigation, these oils came from marine carbonate source rocks that included Type II-S kerogen, and they were deposited under sulfate-reducing circumstances (Al-Khafaji et al., 2018). The Sulaiy Formation has impermeable layers that contribute to oil migration into the Mishrif Formation Reservoir. Migration paths, both vertical and lateral, that created the regional petroleum system control the complete petroleum system in this area (Aqrawi et al., 2010; Al-Khafaji et al., 2018).

3. Methodology

The study wells were selected based on the availability of their data and their ideal distribution in the studied field.

3.1. Samples and data

The Basrah Oil Company (BOC) has not given permission to the authors to reveal well information. Therefore, the locations and names of the wells were encrypted. One hundred and ninety core samples were chosen and distributed to four selected wells (wells 1–4), which are dispersed equally throughout the surveyed Zubair oilfield (Fig. 1); the depth of the samples was corrected using the wireline log depth. The core description was created directly by the BOC organisation, and also used the final geological well reports, well logs, technical reports, and previous studies of the studied wells.

According to Flügel (2010), the environment of the microfacies for the ramp was determined by its place on the shelf. Dunham's classification was used (Dunham, 1962), which was modified by Embry and Kloven (1971), to describe the matrix and grains of the carbonate rocks. Many studies have indicated that the platform of the studied formation was deposited on a ramp instead of a shelf; therefore, the RMF classification of Flugel (Flügel (2010) was used. The most important of those studies are Al-Fares et al. (1998), Mahdi and Aqrawi (2014), Vogel et al. (2016), and Wells et al. (2019).

3.2. Thin section and software

A total of 220 standard thin sections were studied at the laboratory of the BOC, and then at the College of Science, University

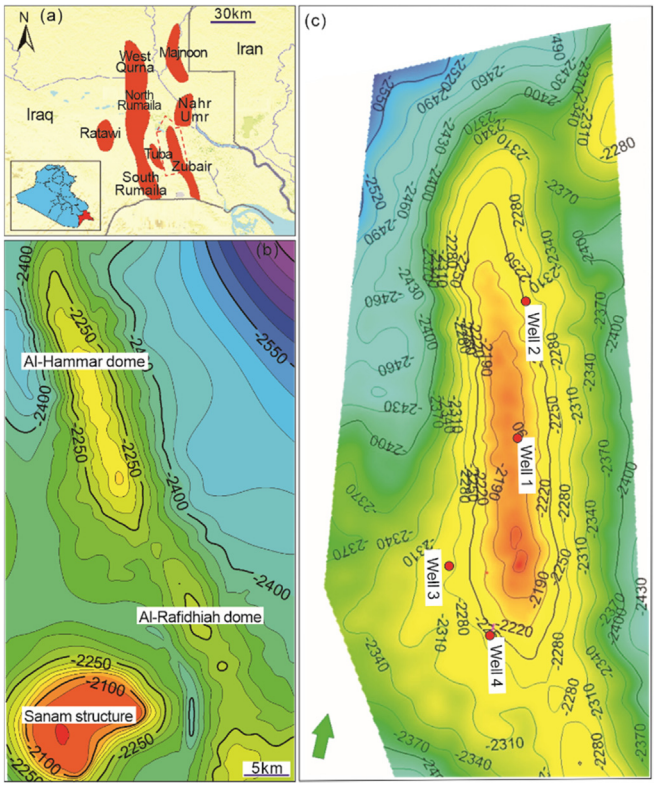

Fig. 1. Location of the study area. (a) The location of the field (Jaffar, 2018), (b) the counter map of the studied formation in the Zubair oilfield (Al-kaabi et al., 2023), and (c) the location of the studied wells in the Al-Rafidiyia dome.

of Basrah to determine the petrography, microfacies, and diagenesis processes. A full set of wireline logs were used for each studied well to enhance the data obtained from thin sections, and the data were interpreted and analysed using Geolog software (Version 17) in the BOC offices. Natural gamma ray, bulk density, and compensated density logs were among the wireline log data gathered for this study. The total gamma ray value represents both the quantity of clay and the radioactivity of the formations (Abdel-Fattah et al., 2022). Analysis of the logs from each of the four wells was performed using current best practices for oil and gas charts (Radwan et al., 2021). Wireline logs are an essential tool for uncovering detailed information on the microfacies; where core data was lost, we were able to check the behaviour of the logs and use them to make a distinction between facies. In this way, some facies were identified and compared with certain cores and vice versa. The sequence stratigraphic approach was based on the integration of all available data, considering the fundamental principles of sequence stratigraphy (e.g., Vail et al., 1977; Posamentier and Vail, 1988).

4. Results

Limestone with a very minor proportion of dolomite is representative of the Mishrif Formation. The lithology of the studied sections is generally as follows. The upper part of the studied formation was composed of light grey limestone with dark grey solution seams and coarse vertical burrows to burrow-mottled, cemented nodules. The middle section contained grey with brown patches, had fine and low angle laminations to tabular cross-bedding, was highly fractured, and had occasional burrowed surfaces and cemented nodules. Rudist and mollusc shells were noticeable, and it was rich in oil evidence. The bottom section was lighter grey coloured, had staff bedding—compacted limestone, and rare sedimentary structures.

4.1. Microfacies of the Mishrif Formation

The study of the formation started with the microfacies. The Mishrif Formation microfacies can be divided into main and secondary microfacies, as described below.

4.1.1. Wackestone microfacies

Wackestone microfacies reflect a shallowing-upward cycle of the formation, and this is the most common microfacies type in the Mishrif Formation. Both the outer ramp and mid-ramp environments contained this microfacies. It was escorted with the packstone microfacies in the transgressive systems tract (TST) and floatstone in the highstand systems tract (HST). Wackestone microfacies can be divided into four submicrofacies, described below.

A Planktonic foraminiferal wackestone submicrofacies W1

This microfacies is characterised by low abundance of skeletal grains (approximately 10%–40% of the rock's component) (Fig. 2A). It contains fossils and fossil fragments with a high percentage of planktonic foraminifera. The most important skeletal grains are calcisphere (*Globotruncana*, *Globigerinelloides, Heterohelix,* and *Hedbergella*) with a low percentage of reef organisms (benthonic), such as algae, bivalves, and echinoderm fragments. These microfacies were correlated with RMF 5, and were located between the middle and outer ramps (Flügel, 2010), representing the deepest microfacies deposited in the Mishrif Formation.

B Miliolids wackestone submicrofacies W2

The benthonic foraminifera are the most common skeletal components in these microfacies, containing small foraminifera with common miliolid (Fig. 2B). Mainly benthic organisms are entrenched in the micrite, as well as some mobile organisms. The micrite contains scattered, often very small skeletal debris, contributing to a fine bioclastic matrix. The typical ramp microfacies is RMF 20, and was deposited within a lagoon environment (Flügel, 2010).

C Pelletal wackestone submicrofacies W3

This submicrofacies is characterised by calcified faecal pellets with distinctive intraclasts; the pellets make up 20% of the total microfacies (Fig. 2C). The submicrofacies appears to fluctuate during the deposition, with the intraclast presenting as clastic crystals. Occasionally, planktonic forms, calcisphere, and framboidal pyrite accompany this microfacies. These submicrofacies, if comparable with ramp microfacies, are located within RMF 9, which represents ramp-derived bioclasts, bounded between the mid-to outer ramp (Flügel, 2010).

D Alveolina wackestone submicrofacies W4

Benthonic foraminifera, peloids, pellets, and calcisiltite make up the largest percentages of the submicrofacies, but the intense spread of the *Alveolina* genera in this submicrofacies is notable (*Dicyclina schlumbergeri*, *Cisalveolina fraasi*, and *Pseudolituonella reichel*). The shape and size of the peloids vary, making up approximately 20% of the total groundmass (Fig. 2D). Different components are also recorded, such as Mollusca shell fragments and calcisiltite matrix. Usually, this submicrofacies occurs at the

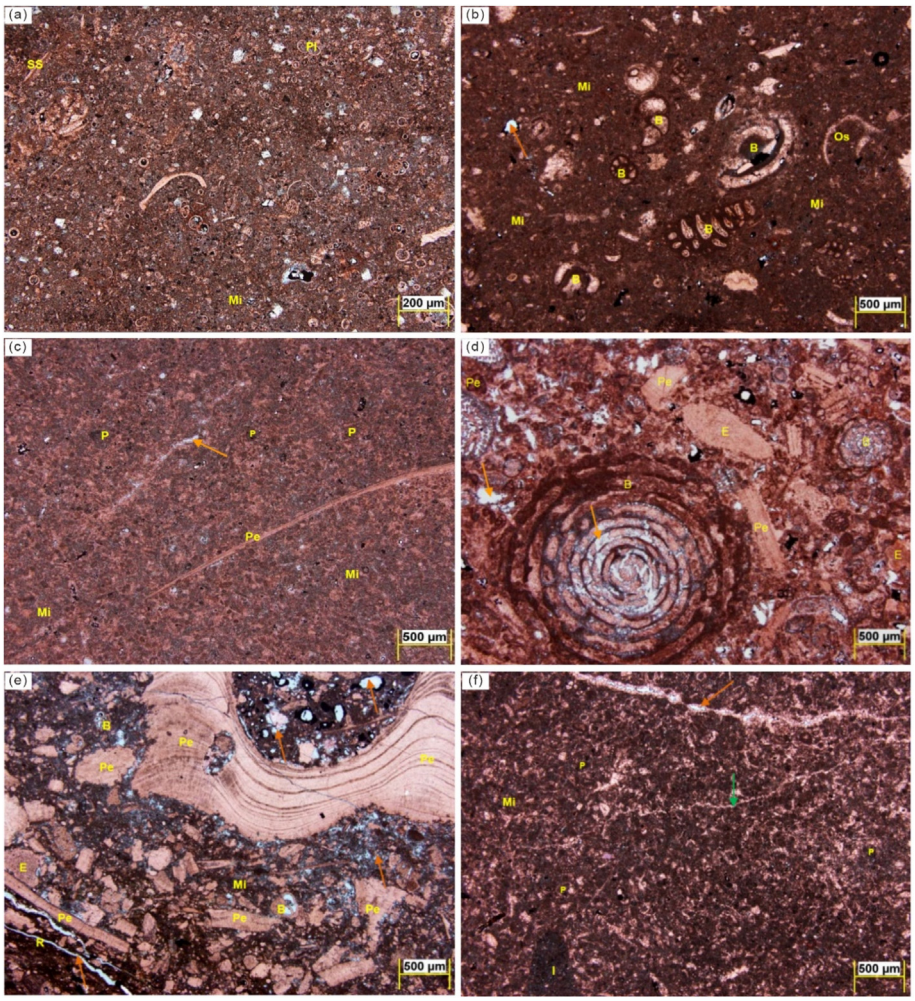

Fig. 2. (A) Planktonic foraminiferal wackestone, enormous numbers of planktonic foraminifera (P) mixed with a few percent of miliolids and calcisphere and sponge spicules; well 1, depth 2352 m, PPL. (B) Miliolids wackestone, benthic organisms (B) (*Nezzazata* sp.) engrained in the micrite (Mi), also ostracods shells (os); well 1, depth 2220 m, PPL. (C) Pelletal wackestone, full of pellets with bivalve shells (Pe); well 2, depth 2330 m, PPL. (D) Alveolina wackestone, *Cisalveolina fraasi*, with fragments of pelecypods and echinoids (E); well 1, depth 2243 m, XPL. (E) Burrowed bioclastic packstone, supported grains of fragmental pelecypods; well 2, depth 2300 m, XPL. (F) Pelletal packstone, micritic groundmass by coalescence of pellets, channel porosity (green arrow); well 2, depth 2235 m, PPL.

deepening stage, with the wackestone microfacies. This submicrofacies is located in the restricted to open inner ramp and represents typical ramp facies of RMF 13 (Flügel, 2010).

4.1.2. Packstone microfacies

The packstone microfacies are characterised by grain support with small spary or micrite matrix bioclast fragments of rudists, bivalves, and benthic foraminifera. This microfacies is common in this formation and is considered the second most important microfacies in the current study. These microfacies can be divided into the following submicrofacies.

A Burrowed bioclastic packstone submicrofacies P1

This microfacies comprises burrowed bioclastic packstone with varied types of common fossils (bivalves, brachiopods, echinoderms) and peloids. Skeletal grains are well preserved (Fig. 2E). The microfacies contain approximately 15–20% allochems, characterised by well-preserved pelecypods belong to different types of pelecypods and rudists. The chambers of some bioclasts are filled partially with micrite. Burrowing indicators are common and many fossils are well preserved. Usually, the channel porosity corresponds with this submicrofacies. The perfect type for this submicrofacies is RMF-3, which presents at the mid-ramp (Flügel, 2010).

B Pelletal packstone submicrofacies P2

The microfacies are mainly composed of a spartic matrix that contains supported small and large bioclasts of foraminifera and limited pelecypods shells with fragments of echinoderm, algae, and ostracods (Fig. 2F). Skeletal grains are worn. It does not contain any type of dissolution or any destructive diagenesis process. These submicrofacies were recorded at the top of the studied formation, and are located within RMF 7, which exists across a wide range from open marine to the mid-ramp (Flügel, 2010).

C Miliolids packstone submicrofacies P3

This microfacies is characterised by an abundance of miliolids and alveolinids with algal bioclast (Fig. 3A). It resembles the miliolids wackestone microfacies but it is grain-supported by miliolid genera, corresponding to RMF 20 (Flügel, 2010). The lagoon environment is a suitable environment for this microfacies, and they are usually located vertically in the upper part of the Mishrif Formation.

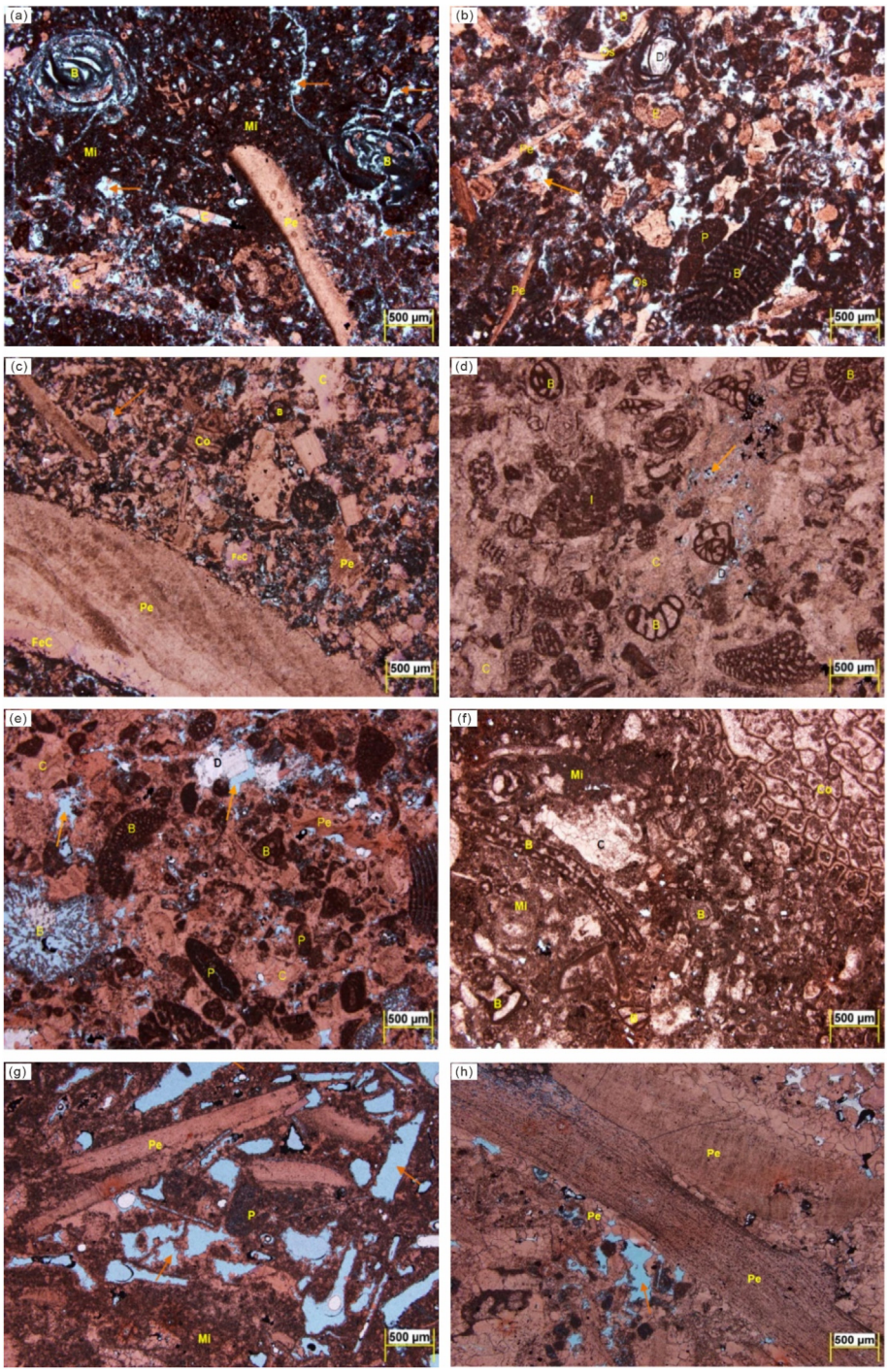

Fig. 3. (A) Miliolids packstone, miliolids genera covered this microfacies, with dispersion of pelecypods fragments and pellets; well 3, depth 2200 m, XPL. (B) Bioclastic grainstone, occupied by echinoderms, bivalves, and rudist fragments, in addition to larger benthonic foraminifera (*Dicyclina schlumbergeri*); well 1, depth 2330 m, XPL. (C) Rudist grainstone, with fragments of coral; well 2, depth 2270 m, XPL. (D) Benthonic foraminiferal grainstone, spiritic groundmass with varied genera of benthonic foraminifera, Nezzazata, miliolids; well 2, depth 2240 m, XPL. (E) Peloidal grainstone, peloids (P) with dispersion pieces of *Dicyclina schlumbergeri*; well 1, depth 2340 m, XPL. (F) Floatstone, coral with number of benthonic foraminifera and algae; well 2, depth 2285 m, PPL. (G) Laminar fenestral bindstone, bivalve shells with peloids, moldic porosity is distinct phenomena in this microfacies; well 1, depth 2200 m, XPL. (H) Dolomite rhombs (Do) accompanied by bindstone microfacies; well 1, depth 2227 m, XPL.

4.1.3. Grainstone microfacies

A Bioclastic grainstone submicrofacies G1

This microfacies is composed of grain-supported bioclasts (60%–70%), foraminifera (planktonic and benthonic, 40%–50%), algae (less than 5%), and another allochem (more than 20%) of the rock that is composed of echinoderms, bivalves, and rudist fragments (Fig. 3B). The alchemical components are cemented by sparry calcite with rough areas of micrite filling the chambers of fossils and spaces, in addition to other skeletal particles. This microfacies represents the deepest facies in the current study, lying

within RMF 8 and typically in a mid-ramp environment (Flügel, 2010). The intensity of grain support is reflected in the high level of energy in the environment.

B Rudist grainstone submicrofacies G2

This submicrofacies is characterised by the dispersion of rudist fragments. It also has different grains: the bioclast grains contain echinoderms, bivalves, benthic foraminifera, and algae (Fig. 3C). Mollusca is an abundant organism at this microfacies, and the groundmass is free of micrite, and is completely sparitic. These submicrofacies are correlated to RMF 8 and a mid-ramp environment (Flügel, 2010).

C Benthonic foraminiferal grainstone submicrofacies G3

This microfacies consists mainly of skeletal particles and sparry calcite as cement. The miliolids are the main component of the skeletal particles, including *Nezzazata* sp., and the binding material between the skeletal particles is sparry calcite cement (Fig. 3D). These microfacies are within RMF 26 and located in a shoal environment (Flügel, 2010).

D Peloidal grainstone submicrofacies G4

Peloids are rather small, subspherical, poorly sorted, sometimes ovoidal in shape, and have no discernible structure. Generally, peloids are present as primary constituents (60%). There are larger foraminifera (*Dicyclina schlumbergeri*), pelecypods, ostracods, and echinoids. The groundmass is spiritic, containing interporosities between grains (Fig. 3E). The presence of peloids and other grains point to a low energy, which could reflect an intertidal environment deposition (Bathurst, 1975).

4.1.4. Floatstone F

The larger size of these fossils is a good indicator of this microfacies. The groundmass of floatstones is micrite-supported carbonate rocks and yields more than 50% grains larger than 2 mm. The larger skeletal component presents a different type of organism, but mostly consists of rudist shells, which form approximately 80% of the submicrofacies, as well as some algae, coral, and sometimes larger foraminifera (Fig. 3F). Usually, this microfacies is deposited in a reef derived from the shoal environment within RMF 28 (Flügel, 2010).

4.1.5. Laminar fenestral bindstone B

This microfacies consists of tightly packed pellets and bivalve shells, and compared with the nearby grain-supported fabric, the porosity is greater (Fig. 3G). Some of the porosity is filled with dolomite. Vadose meteoric calcite is used to fill the moulds of previous dolomite rhombs (Fig. 3H). This submicrofacies represents the shallowest basin during the history of the Mishrif deposition within RMF 23, and is deposited in an intertidal environment.

4.2. Depositional environment

Depending on the main and secondary microfacies, this study covers several environments.

4.2.1. Mid-ramp environment

The mid-ramp environment represents the deepest environment in the Mishrif Formation. It is epitomised by the lower part of Mishrif Formation associations. Mid-ramp deposits contain bioclasts fragments, peloids, wackestone, wacke-packstone with very minor floatstone, grainstone, and boundstone. The proximal part of the mid-ramp environment contains the skeletal fragments as common bioclasts but are not highly abundant, whereas the distal part of the mid-ramp environment has fewer skeletal fragments but with abundant planktonic foraminifera.

The bioclast fragments are always debris of pelecypods, gastropods, green algae, rudists, echinoderms, and benthic foraminifera. The distal part of the mid-ramp environment included dominant and common fine grain, wackestone, wackestone-packstone, and argillaceous. This environment exhibits a cleaning-upward trend and enhanced facies characterised by argillaceous wackestone in the distal section, progressing from a clean-up section to more a grain-rich wackestone-packstone and packstone in the proximal part.

These trends may be gradually overlaid by the cleaner and grainier shoal deposits, often overlaid by mid-ramp deposits. The wackestone and wackestone-packstone are dominant textures in the mid-ramp microfacies. The energy level ranges from low to moderate. The low diversity and richness of macrofauna and uniformly bedded and highly bioturbated nature are the best indicators of open marine conditions (Flügel, 2010). The continuous facies belt is an attribute of mid-ramp associations within the depositional system. The wireline response of the mid-ramp deposits is not uniform or constant, but the value of the gamma rays is less than the value of lagoon associations because there is more argillaceous lithofacies of the mid-ramp minor than in lagoon, the density log is mainly of intermediate value, and uniform when the gamma ray is uniform.

4.2.2. Shoal environment

This microfacies has peloidal skeletal packstone to grainstone rudist attitudes, and floatstone and rudstone are considered the shoal environment facies. The grains are moderately sorted to well-sorted. The bioclasts of the shoal environments are bivalves, intraclasts, corals, green algae, echinoderms, and rudist shells. The shoal is characterised by moderate to high-level energy conditions (Almohsen, 2019). Echinoderms are the common grains in a shoal with a cleaning-upward trend, are well-sorted, and have small intervals of dirtier uptrend. The texture and bioturbated fabric associated with these shoal facies are imitated inner shoal settings where the sediment surface was stable (Ismail et al., 2021).

The wireline log response of shoal facies successions has a comparatively uniform and lower gamma ray value caused by the high energy level. Shoal deposits have uniform lithology, which builds up this succession, and better porosity because of greater macropore components; they typically have low-density log value and high neutron porosity log value.

4.2.3. Lagoon environment

The lagoon environment is characterised by skeletal peloid wackestone, wacke-packstone, and packstone fabric. Low assemblages of fauna contain benthic foraminifera, including miliolids, thin shell bivalves, rudist fragments, and green algae, which are rarely abundant in lagoon environments. A low to moderate energy level marks the lagoon association (El-Moghny and Afifi, 2022). A lagoon environment has a higher energy level and is cleaner when equivalent with intertidal facies and has a lower energy and is dirtier when equivalent with shoal. The wireline log response of the lagoon facies has an elevated gamma ray level because of the preservation of organic materials. The log value generally increased while the neutron porosity log decreased because lagoon facies have tighter fabric, fewer open pore space, and are more disposed to the cementation process, which is defined as early cement (Almohsen, 2019).

4.2.4. Intertidal environment

The intertidal environment facies represent the shallowest water depositional setting in the Mishrif Formation. Intertidal facies are dominated by bioturbated skeletal wackestone and rare packstone facies, interbedded skeletal packstone with wackestone and argillaceous prone wackestone, low accumulation of benthic foraminifera, thinly shelled bivalves, and reworked skeletal debris. These facies are consistent with low-energy settings. The accumulation of bioturbated wackestone indicated less restriction and increased oxygen in the water column to support burrowing organisms. Tides, sporadic storms, and marine flooding events reflected high energy reworking into settings and were often followed by periods of low sedimentation rate (Anell et al., 2021). The intertidal facies refer to the accumulation of the lower energy level and grain-poor wackestone and packstone with finely interbedded argillaceous units. Argillaceous material source is fluvial and transported many kilometres, but not a marker for fluvial processor coarse grain siliclastic materials. Intertidal successions are measured to refer to a more proximal area landward comprising lagoon successions, which gradationally inter-finger laterally and vertically with intertidal facies.

4.3. Sequence stratigraphy

A number of references are referred to in this study for the division of sequence stratigraphy (Catuneanu, 2006, 2017; Catuneanu et al., 2009, 2011; Miall, 2013). The sequence stratigraphy of the Mishrif Formation refers to two regression cycles. The lower maximum flooding surface (K-135) was defined by Aqrawi et al. (2010), while the other maximum flooding surface (K-140) was identified by Sharland et al. (2001) and represents the upper part of Arabian Plate megasequence. Two third-order depositional sequences were identified in the Mishrif Formation within the study area. With the exception of S1, the sequences are made up of transgressive–regressive (T-R) cycle sets. All of the cycles are asymmetric, and the regressive phase is dominant. Transgressive cycles have been interpreted as TSTs while regressive cycles are HSTs; maximum flooding surfaces (MFSs) represent turning points between transgression and regression. These cycles or sequences have varying durations because of variations in eustacy, tectonism, climate, and other processes occurring within depositional environments.

Transgressive cycles (TST) are characterised by deep-marine facies dominated by pelagic wackestone. An increasing abundance of planktonic foraminifera is interpreted as indicating a deepening event, which may culminate with the development of a unit in sequences. These shale units have widespread distribution and are recorded in oilfields. Regressive cycles (HST) are characterised by an increasing abundance of benthic fossils and a net volume of grain-dominated facies. This change is reflected in well log signatures, which show a gradual increase in sonic profiles and decrease in gamma ray profiles (de Mello e Silva et al., 2019). In some cases, two separate successions can be identified within an HST. The lower succession corresponds to an early-phase highstand (EHST) consisting of deep-marine and shallow-shelf open marine facies in inner-shelf settings; EHST deposits are characterised by mud-rich lagoonal facies with or without thin rudist lithosomes. The overlying succession represents later HST deposits (LHST) composed of higher-energy shallow-shelf open-marine facies overlain by microbial facies and rudist-rich and lagoonal facies.

4.3.1. Mishrif sequence 1

SB1: This sequence boundary is located at the bottom of the Mishrif Formation and corresponds to the characteristic top of density peak log and low porosity.

MF1: Located in the base of high-density log and with low acoustic log value.

This sequence, marked SB type 2, is at the top of the Rumaila Formation, the equivalent of the lower unit of the Mishrif Formation. It has microfacies and gamma ray wireline data values ranging between 20 and 30 GAPI for both TSTs and HSTs. Abundant planktonic foraminifera were present among the TST. The HST microfacies included sessile bivalves, sponge speckles, and fragments of echinoderms and rudists. The porosity properties values increased in the HST because of the enhanced microfacies properties (Mahdi et al., 2022a). The microfacies presents planktonic foraminifera wackestone in a TST to packstone and grainstone in the upper part of the HST.

4.3.2. Mishrif sequence 2

SB2: Top of the gamma ray interval and density peak, with the appearance of planktonic foraminifera microfacies.

MF2: Increasing in gamma ray and low-density value with benthic foraminifera microfacies.

This sequence is equivalent to the lower part of the middle section of the Mishrif Formation. This sequence is marked by high heterogeneity of lagoonal and shoal facies. The TST contains local marine flooding marks, and the facies indicate a shoal environment. The HST marked when the environment changed to lagoonal and benthic foraminifera became abundant.

4.3.3. Mishrif sequence 3

SB3: Located in the base of a clean gamma ray interval with shoal microfacies.

MF3: At the top of a clean gamma ray interval with a benthic foraminifera appearance.

This sequence is equivalent to the upper part of the middle Mishrif Formation unit. This sequence is characterised by low gamma ray and density values for the TST because of the shoal depositional environment. A dirtying upward trend was observed in the gamma ray value and an increase in density log values was seen during the HST. The microfacies of the TST are characterised by packstone and grainstone (rudist fragments, echinoderms, and coral). According to maximal gamma ray log values, the shale units correlate to the peak transgression and MFS (Mahdi and Aqrawi, 2014). The HST environment changed to a lagoon environment, and benthic foraminifera are the common bioclast microfacies in the HST.

4.3.4. Mishrif sequence 4

SB4: High gamma ray peak and high-density log correlated to the cap rock II (CRII).

MFS140: This surface correlated with the MFS, defined by Sharland et al. (2001), and is characterised by planktonic foraminifera; the wireline gamma ray is marked with a peak of gamma rays.

Sequence 4 is equivalent to CRII and the lower part of the upper Mishrif Formation. Regional maximum flooding covers the field after the regressive at the end of sequence 3. The sequence boundary at the top of CRII is marked by a high-density log and gamma ray peak and planktonic foraminifera. This MFS correlated with the maximum flooding of K-140, which was identified by Sharland et al. (2001). The TST microfacies have planktonic foraminifera and mid-ramp facies characters. In this section, the gamma ray values increase and the shoal facies were capped by lagoon facies, and the argillaceous increased because of the regression of the sea level.

4.3.5. Mishrif sequence 5

SB5: A high gamma ray and base high-density interval value

with planktonic foraminifera microfacies.

MF5: Low gamma ray point and base of the low-density log value with shoal microfacies above.

This sequence includes the upper part of the upper Mishrif Formation, extending to the unconformity surface that was marked as a regional unconformity. The TST showed planktonic foraminifera microfacies with a low-porosity interval and high-density values, while the HST marked when the microfacies reflected the shoal facies. The environment changes from a shoal to lagoon environment in the HST, and the upper part of the environment reached an intertidal environment containing rare fossils.

5. Discussion

The carbonate ramp stratigraphy is suggested for the interpretation of the current microfacies, and is composed of various depositional systems (outer ramp, mid-ramp, and inner ramp) (Sadooni and Aqrawi, 2000; Aqrawi et al., 2010). Facies analysis included the identification of important surfaces (such as subaerial exposure surfaces and MFSs), and facies correlation was based on the definition of sedimentary surfaces having stratigraphic relevance. The full description of the various facies' types and their interpretation in terms of depositional settings constitutes the first stage. The Mishrif Formation was deposited on the eastern Arabian carbonate platform inside the Tethyan Realm (Jassim and Goff, 2006).

The deposition of the studied formation was affected by important factors: the eustacy of the sea level and tectonic processes with environmental influences. In this discussion, we will trace the most important of these events. The high-resolution sequence stratigraphy of the Mishrif Formation, presented in Figs. 4–6, depends on the Arabian Plate sequence stratigraphy framework. Because it is closely related to petroleum geology and has an impact on the development of petroleum system components, Iraq's tectonic history has influenced changes in stratigraphy and facies over time, as well as the development of unconformities, onlap geometries, tectonic divisions, subdivisions, and present-day paleostructural elements (Abdel-Fattah et al., 2022; Mahdi et al., 2022b).

The studied formation of the investigated subsurface structures was influenced by the salt mechanism, basement uplift, and Hercynian orogeny. The Zubair subzone is affected by strike-slip faults as a result of the shear stress of the Arabian Plate's rotation (Al-Kaabi et al., 2023) and the continuous growth of the same structures since the early Jurassic or early Cretaceous to the present (Al-Sakini 1992).

The facies of the Mishrif Formation and the reservoir quality are both influenced by local and regional tectonics (Aqrawi et al., 2010). For most of the early Cretaceous, Halokinitric tectonism played a modest influence in controlling of sedimentation, but in the late Albian (for example), tectonism became more apparent because of potential basement fault activation and relative block displacement along with the salt diaprism (Sadooni and Aqrawi, 2000; Aqrawi et al., 1998).

This study framework depends on core description, microfacies analysis, and wireline logs to predict fourth-order sequence stratigraphy parasequences. The Mishrif Formation in this study contains five fourth-order sequence stratigraphy parasequences. The formation consists of bedded limestone with a variety of types of fossils, such as algae, benthonic and planktonic foraminifera, echinoderms, and burrowed bivalves. The environment of deposition gradually transitions from mid-ramp to intertidal, indicating a regression depositional cycle. At the upper part of the Mishrif Formation, the chosen regional MFS K-140 depends on microfacies plates and wireline log data, such as gamma rays and density logs.

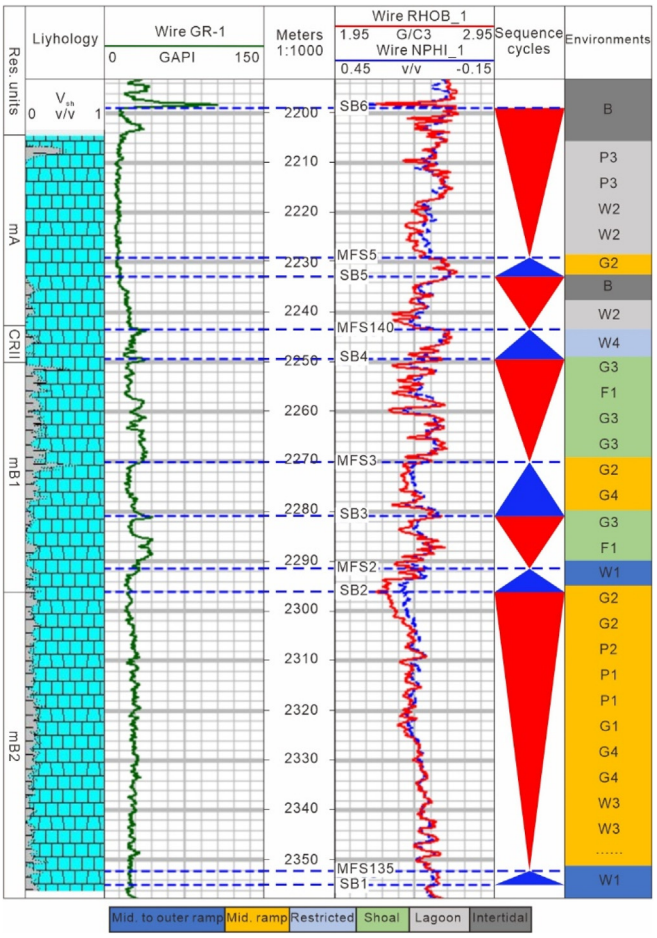

Fig. 4. Sequence stratigraphy of the Mishrif Formation at Well 1; microfacies and environmental interpretation are provided for convenience. SB: sequence boundary, MFS: maximum flooding surface, Res: reservoir.

Another regression cycle is shown above the K-135 surface. This cycle contains two parasequences before the unconformity surface, which is defined as the border between the Mishrif and Khasib Formations. This study's results on the K-135 and K-140 (Figs. 4–6) agree with those of Aqrawi et al. (2010), Sharland et al. (2001), Mahdi et al. (2013), and Mahdi and Aqrawi (2014), but do not record results for K-130, as in the mentioned studies. Two important studies in the field of sequence stratigraphy of the Mishrif Formation are Mahdi and Aqrawi (2014) and Awadeesian et al. (2015), both of which consider the base of the Mishrif Formation to start with the HST; however, the current study considers the formation to start with the TST. All of the studied wells begin with planktonic foraminifera with deep environment reaches to the outer ramp. Below the Mishrif Formation lies the Rumalia Formation, ending in the shallow environment (shoal) (Mahdi et al., 2022a); therefore, the Mishrif Formation represents a transgressive cycle. The Mesopotamian plain was situated in the humid tropics (5–10°N) during the Albian and Cenomanian, while during the Cretaceous period it was situated between 2 and 3°N of equivalence. The Cretaceous period was a greenhouse cycle and included one of the warmest stages of the earth's geologic history (Cenomanian) (Schlanger and Jenkyns, 1976; Al-Sherwani, 1983). There was a significant increase in sea level during the Cenomanian age (96 MY) (Haq et al., 1987), but as the cycles were ended with regional unconformity, the continuity of the secondary Hercynian movements caused a retreat of sea level, which led to exposure and erosion of the Mishrif facies

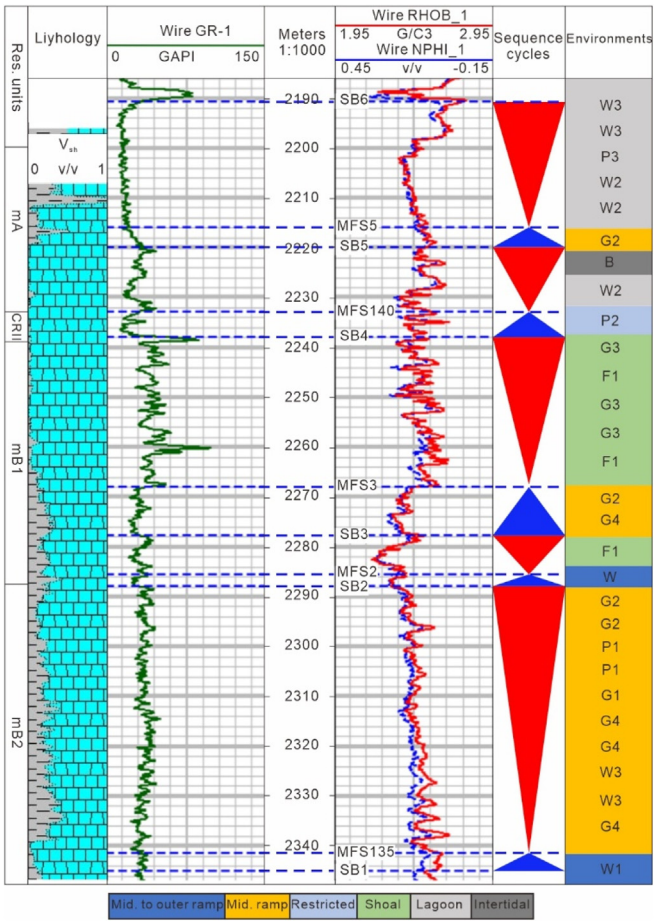

Fig. 5. Sequence stratigraphy of the Mishrif Formation at Well 2; microfacies and environmental interpretation are provided for convenience. SB: Sequence boundary, MFS: maximum flooding surface, Res: reservoir.

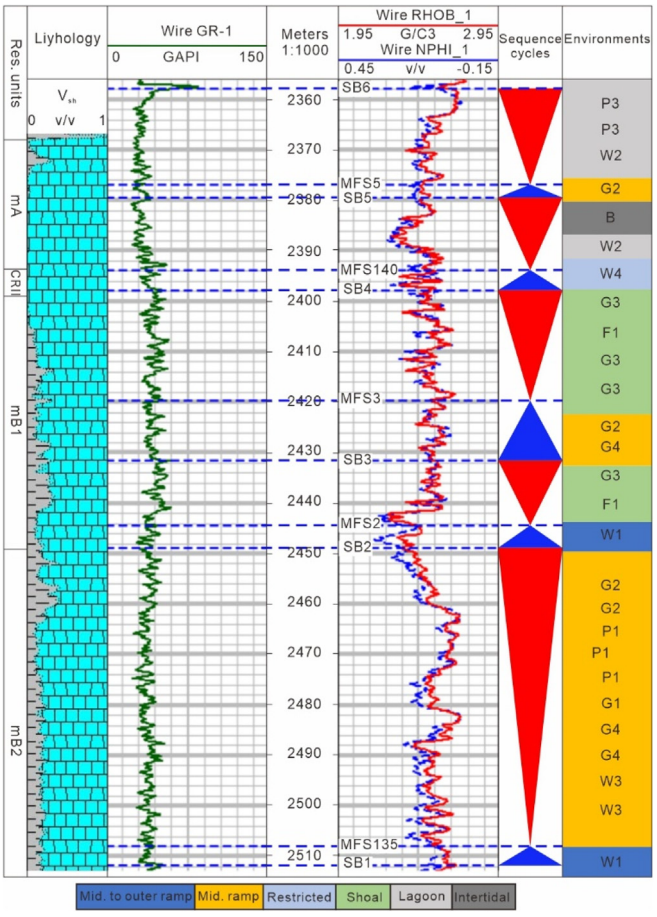

Fig. 6. Sequence stratigraphy of the Mishrif Formation at Well 3; microfacies and environmental interpretation are provided for convenience. SB: Sequence boundary, MFS: maximum flooding surface, Res: reservoir.

with unconformable beds of conglomerates between the Mishrif and Khasib Formations (Al-Khersan, 1975; Handhel, 2006).

Increasing the cost of oil exploration requires the use of effective and inexpensive means to search for places of hydrocarbon gatherings and discover unnoticed traps. These hydrocarbon gatherings are associated with facies distributions laterally and vertically through geological time. Because the sequence stratigraphic framework provides the limiting boundaries within which data are distributed away from wells into the interwell area, it is essential for successfully characterising carbonate reservoirs. BOC has divided the Mishrif Formation into several reservoir units: CRI (cap rock-1), m A (main bay A), CRII (Cap rock-2), mB1 (main bay 1), and mB2 (main bay-2) (Mahdi and Aqrawi, 2014). The results of the current study (Figs. 4–6) show that the hydrocarbon accumulation in the first sequence was low because of the low-porosity and high-density limestone, the hydrocarbon increased in the late HST, and the second and third sequences had good hydrocarbon accumulation because of the change in the depositional environment to a shoal environment with high porosity values. Rare hydrocarbon content increased in the early fourth systems tract because of the transgressive that occurred until the MFS 140, whereas the content decreased during the fourth sequence highstand and the transgressive fifth sequence because of the improved depositional environment. The hydrocarbon accumulation decreased in the late HST of the fifth sequence indicated by increasing density log values and caused by the environment changing to a restricted lagoon environment.

6. Conclusions

The carbonate Mishrif Formation consists of a variety of limestone that reflects depositional environments. The Mishrif Formation deposits in shallow marine environments, which progress from the lower to upper parts of the formation from mid-ramp, shoal, lagoon, and intertidal environments. This study describes five main microfacies: wackestone, packstone, grainstone, floatstone, and bindstone. Rudists, benthic foraminifera, echinoderms, burrows, and algae are the common microfacies in the Mishrif Formation. The microfacies and wireline log data used in this study indicate that the formation consists of two regression cycles. The depositional sequence of the Mishrif Formation includes five parasequences of T-R cycles. In the first parasequence, the MFS K-135 is located in the lower part of the Mishrif Formation. The microfacies grade up because of shallowing-upward and the changing environment to a shoal environment. The MFS K-140 is in the upper part of the Mishrif Formation. The parasequence reflects the eustatic sea-level change in the Cenomanian–Turonian period and the accommodation space development of shallow marine, which is punctuated by exposed surfaces caused by sea level falls between the Mishrif Formation and the overlying Khasib Formation. The distribution of the reservoir, source, and seal facies for each particular sequence can be predicted using the T-R sequences' temporal framework. This is crucial for exploration and production events. The low porosity and high density of the limestone in the first sequence result in low hydrocarbon accumulation.

Hydrocarbon accumulation increased in the late HST, and the second and third sequences had good hydrocarbon accumulation because the depositional environment had changed to a shoal environment with high porosity. Caused by a transgression, the rare hydrocarbon content increased in the early fourth systems tract, whereas the content was reduced because of the enhanced depositional environment in the fourth sequence highstand and the transgressive fifth sequence.

Declaration of competing interest

The authors declare no conflict of interest.

References

Abdel-Fattah, M.I., Mahdi, A.Q., Theyab, M.A., Pigott, J.D., Abd-Allah, Z.M., Radwan, A.E., 2022. Lithofacies classification and sequence stratigraphic description as a guide for the prediction and distribution of carbonate reservoir quality: a case study of the Upper Cretaceous Khasib Formation (East Baghdad Oilfield, Central Iraq). J. Petrol. Sci. Eng. 209, 109835.

Al- Rubiay, H.F., 2009. Sequence Stratigraphy of the Mishrif Formation at West Qurnah North Rumaila, and Zubair Fields Southern Iraq (B.Sc. Thesis). University of Baghdad, Baghdad, p. 126.

Al-Ali, M., Mahdi, M.M., Alali, R., 2019. Microfacies and depositional environment of Mishrif Formation, North Rumaila oil field, southern Iraq. Iraqi Geological Journal 52 (2), 91–104.

Al-Ameri, T.K., Al-Khafaji, A.J., Zumberge, J., 2009. Petroleum system analysis of the Mishrif reservoir in the ratawi, Zubair, north and south Rumaila oil fields, southern Iraq. GeoArabia 14 (4), 91–108.

Al-Dulaimy, R.T., 2010. Biostratigraphy of the Mishrif Formation from Halfayah-1, Amarah 1, and Majnoon Oilwells Southern Iraq (M.SC Thesis). University of Baghdad, Baghdad, p. 134.

Al-Fares, A.A., Bouman, M., Jeans, P.A., 1998. New look at the middle to lower cretaceous stratigraphy. Offshore Kuwait. GeoArabia 3 (4), 543–560.

Al-Jafar, M., Al-Jaberi, M., 2019. Well logging of Zubair formation for upper sandstone member in Zubair oilfield, southern Iraq. Iraqi Geological Journal 52 (1), 101–124.

Al-Kaabi, M., Hantoosh, D., Neamah, B., Almohy, H., Bahlee, Z., Mahdi, M., Abdulnaby, W., 2023. The structural analysis of the oilfields in Zubair subzone, Southern Iraq. Afr. J. Earth Sci. 197, 104770.

Al-Khafaji, A.J., Hakimi, M.H., Najaf, A.A., 2018. Organic geochemistry characterization of crude oils from Mishrif reservoir rocks in the southern Mesopotamian Basin, South Iraq: implication for source input and paleoenvironmental conditions. Egyptian J. Petrol. 27 (1), 117–130.

Al-Maliki, H.S., 2009. Geological and Reservoir Assessment of Mishrif Formation in West Qurna Field, South Iraqi Oil Fields (M.SC Thesis). University of Basrah, Basrah, p. 156.

Al-Mutury, W.G., Al-Asadi, M.M., 2008. Tectonostratigraphic history of mesopotamian passive margin during mesozoic and cenozoic, South Iraq. J. Kirkuk Univ. 3, 31–50.

Al-Mutury, W.G., Al-Mayahi, D.S.B., 2010. Geometric and genetic structural analysis of Zubair oil field, southern Iraq. Qadissya Sci. 3, 89–97.

Al-Najm, F.M., 2013. Mesopotamian Basin Evolution and Reservoir Characterization of the Mishrif Formation at Selected Fields, South and South Eastern Iraq (Ph.D. Thesis). University of Basrah, Basrah, p. 234.

Al-Sakini, J., 1992. Summary of the Petroleum Geology of Iraq and the Middle East. Northern Oil Company Press, Kirkuk, p. 179.

Al-Sharhan, A.S., Nairn, A.E.M., 1988. A review of the cretaceous formations in the arabian peninsula and gulf-part II: mid-cretaceous (Wasia Group) stratigraphy and paleogeography. J. Petrol. Geol. 11, 89–112.

Al-Sherwani, G.H., 1983. Depositional Environments and Stratigraphic Relationships of Mishrif Formation in Selected Boreholes, Central and Southern Iraq (M.Sc. Thesis). University of Baghdad, Baghdad.

Al-Sherwani, G.H., 1988. Lithostratigraphy and environmental considerations of cenomanian- early turonian shelf carbonates (Rumaila and Mishrif Formation) of Mesopotamian basin. AAPG Bull. 71, 614.

Al-Khersan, H., 1975. Depositional Environments and Geological History of the Mishrif Formation in Southern Iraq. 9th Arab Petroleum Congress, Dubai.

Almalikee, H.S., Souvik, S., 2021. Present-day stress field and stress path behaviour of the depleted Mishrif reservoir from the super-giant Zubair oilfield, Iraq–A geomechanical case study. J. Afr. Earth Sci. 184, 104381.

Almohsen, M.J., 2019. Facies Architecture, Clay Minerals and its Effect on Petrophysical Properties of Mishrif Formation in West Qurna Oilfield Southern Iraq (MSc Thesis). University of Basrah, Basrah, p. 202.

Anell, I., Zuchuat, V., Röhnert, A., Smyrak Sikora, A., Buckley, S., Lord, G., Maher, H., Midtkandal, I., Ogata, K., Olaussen, S., Osmundsen, P., Braathen, A., 2021. Tidal amplification and along-strike process variability in a mixed-energy paralic system prograding onto a low accommodation shelf, Edgeøya, Svalbard. Basin Res. 33 (1), 478–512.

Aqrawi, A.A.M., Horbury, A.D., 2008. Predicting the Mishrif reservoir quality in the Mesopotamian basin, southern Iraq. GeoArabia Abstract 13 (1), 127–128.

Aqrawi, A.A.M., Thehni, G.A., Sherwani, G.H., Kareem, B.M.A., 1998. Mid-Cretaceous rudist-bearing carbonates of the Mishrif Formation: an important reservoir sequence in the Mesopotamian Basin, Iraq. J. Petrol. Geol. 21 (1), 57–82.

Aqrawi, A.A., Goff, J.C., Horbury, A.D., Sadooni, F.N., 2010. The Petroleum Geology of Iraq. Scientific Press Ltd, Beaconsfield, p. 424.

Awadeesian, A.M., Al-Jawed, S.N., Saleh, A.H., Al-Sherwani, G.H., 2015. Mishrif carbonates facies and diagenesis glossary, South Iraq microfacies investigation technique: types, classification, and related diagenetic impacts. Arabian J. Geosci. 8 (12), 10715-10373.

Bathurst, R.G.C., 1975. Development in Sedimentology 12, Carbonate Sediments and Their Diagenesis, second ed. Elsevier Pub. Co., Amsterdam, p. 658.

Buday, T., Jassim, S., 1987. The Regional Geology of Iraq, Vo.2: Tectonism, Magmatism and Metamorphism. Geosurv, Baghdad, p. 352.

Catuneanu, O., 2006. Principles of Sequence Stratigraphy. Elsevier.

Catuneanu, O., 2017. Sequence stratigraphy: guidelines for a standard methodology. Stratigr. Timescales 2, 1–57.

Catuneanu, O., Abreu, V., Bhattacharya, J.P., Blum, M.D., Dalrymple, R.W., Eriksson, P.G., Fielding, C.R., Fisher, W.L., Galloway, W.E., Gibling, M.R., Giles, K.A., 2009. Towards the standardization of sequence stratigraphy. Earth Sci. Rev. 92 (1–2), 1–33.

Catuneanu, O., Galloway, W.E., Kendall, C.G.S.C., Miall, A.D., Posamentier, H.W., Strasser, A., Tucker, M.E., 2011. Sequence stratigraphy: methodology and nomenclature. Newsl. Stratigr. 44 (3), 173–245.

Chatton, M., Hart, E., 1961. Review of the Cenomanian to Maastrichtian Stratigraphy in Iraq. INOC Library, Baghdad, p. 23.

Dunham, R.J., 1962. Classification of carbonate rocks according to depositional texture. AAPG Memoir 1, 108–121.

El-Moghny, M., Afifi, A., 2022. Microfacies analysis and depositional environments of the middle eocene (bartonian) qurn formation along qattamiya—ain sokhna district, Egypt. Carbonates Evaporites 37 (18), 3–16.

Embry, A.F., Kloven, J.E., 1971. A late devonian reef tract on northeastern banks island, northwest territories. Bull. Can. Petrol. Geol. 19, 730–781.

Flügel, E., 2010. Microfacies of Carbonate Rocks, second ed. Springer, Heidelberg, p. 1006.

Fouad, S.F., 2015. Tectonic map of Iraq, scale 1: 1000 000, 2012. Iraqi Bulletin of Geology and Mining 11 (1), 1–7.

Handhal, A., Mahdi, M., 2016. Basin modeling analysis and organic maturation for selected wells from different oil fields, Southern Iraq. Model. Earth Syst. Environ. 189 (2), 1–14.

Handhel, A.M., 2006. Study of reservoir characteristic for Mishrif Formation. In: Nassyria Oilfield and Their Relationship with Oil Productivity (M.Sc. Thesis). University of Basrah, Basrah, p. 166.

Haq, B.U., Hardenbol, J., Vail, P.R., 1987. Chronology of fluctuating sea levels since the Triassic. Science 235, 1156–1167.

Ismail, M.J., Ettensohn, F.R., Handhal, A.M., Al-Abadi, A.M., 2021. Facies analysis of the Middle Cretaceous Mishrif Formation in southern Iraq borehole image logs and core thin-sections as a tool. Mar. Petrol. Geol. 133 (2), 105324.

Jaffar, H.M., 2018. Structural Geology of Rumaila Oilfield in Southern Iraq from Well Logs and Seismic Data (Msc. Thesis). University of Basrah, Basrah, p. 104.

Jassim, S.Z., Goff, J., 2006. Geology of Iraq. Dolin, Prague and Moravian Museum, Berno, p. 332.

Mahdi, T.A., Aqrawi, A.A.M., 2014. Sequence stratigraphic analysis of the mid-cretaceous Mishrif Formation, southern Mesopotamian basin, Iraq. J. Petrol. Geol. 37 (3), 287–312.

Mahdi, T.A., Aqrawi, A.A., Horbury, A.D., Al-Sherwani, G.H., 2013. Sedimentological characterization of the mid-Cretaceous Mishrif reservoir in southern Mesopotamian Basin, Iraq. GeoArabia 18 (1), 139–174.

Mahdi, L.A., Mahdi, M.M., Handhal, A.M., 2021. Determination of the best reservoir units for Upper Shale Member of the Zubair Formation by using several petrophysical properties, Southern Iraq. Misan J. Acad. Stud. 41, 174–193.

Mahdi, M., Ismail, M., Mohammad, O., 2022a. The integration of wireline logs and sedimentological data to predict sequence stratigraphic framework in carbonate rocks: an example from Rumaila Formation (Cenomanian), West Qurna Oil Field, Southern Iraq. Stratigr. Geol. Correl. 30 (5), 360–377.

Mahdi, A.Q., Abdel-Fattah, M.I., Hamdan, H.A., 2022b. An integrated geochemical analysis, basin modeling, and palynofacies analysis for characterizing mixed organic-rich carbonate and shale rocks in Mesopotamian Basin, Iraq: insights for multisource rocks evaluation. J. Petrol. Sci. Eng. 216, 110832.

Miall, A.D., 2013. Principles of Sedimentary Basin Analysis. Springer science & Business Media, p. 380.

Owen, R.S., Nasr, S., 1958. The stratigraphy of the Kuwait-Basrah area. In: Weeks, G.L. (Ed.), Habitat of Oil a Symposium. AAPG, Tulsa.

Posamentier, H.W., Vail, P.R., 1988. Eustatic controls on clastic deposition II-sequence and systems tract models. In: Wilgus, C.K., Hastings, B.S., Kendall, C.G.StC., Posamentier, H.W., Ross, C.A., Van Wagoner, J.C. (Eds.), Sea Level Changes: an Integrated Approach, vol. 42. SEPM Spec. Publ., pp. 125–154

Powers, R.W., 1962. Arabian upper Jurassic carbonate reservoir rocks. In: Ham, W.E. (Ed.), Classification of Carbonate Rocks: a Symposium, vol. 1. AAPG Memoir, pp. 122–192.

Rabanit, P.M.V., 1952. Rock Units of Basrah Area. BPC.

Radwan, A.E., Abdelghany, W.K., Elkhawaga, M.A., 2021. Present-day in-situ stresses in Southern Gulf of Suez, Egypt: insights for stress rotation in an extensional rift basin. J. Struct. Geol. 147 (7), 104334.

Razoian, A.M., 2002. A Study to Improve Enhanced Oil Recovery of Mishrif Reservoir

in North Rumaila and West-Qurna and Main Pay in South Rumaila Fields (MSc Thesis). University of Basrah, Basrah, p. 145.
Sadooni, F.N., Aqrawi, A.A., 2000. Cretaceous sequence stratigraphy and hydrocarbon potential of the Mesopotamian Basin, Iraq. In: Alsharhan, A.S., Scott, R.W. (Eds.), Middle East Models of Jurassic/Cretaceous Carbonate Systems, vol. 69. SEPM Special Publication, pp. 315–334.
Schlanger, S.O., Jenkyns, H.C., 1976. Cretaceous oceanic anoxic events: causes and consequences. Geol. Mijnbouw 55, 179–184.
Scott, R.W., 1990. Global environmental controls on Cretaceous reefal ecosystems. Palaeogeogr. Palaeoclimatol. Palaeoecol. 119, 187–199.
Sharland, P.R., Archer, P.R., Casey, D., Davies, R., Hall, S., Heward, A., Horbury, A., Simmons, M., 2001. Arabian Plate Sequence Stratigraphy, vol. 2. GeoArabia Special Publication, Bahrain, p. 372.
Silva, F.E., Beneduzi, C., Nassau, G., 2019. Using sonic log to estimate porosity and permeability in carbonates. In: 16th International Congress of the Brazilian. Geophysical Society, pp. 1–6.
Vail, P.R., Mitchum, R.M., Thompson, S., 1977. Global cycles of relative changes of sea level. In: Payton, C.E. (Ed.), Seismic Stratigraphy Application to Hydrocarbon Exploration, vol. 26. AAPG Mem, pp. 23–97.
Vogel, K., Edward, J., Shell, F., 2016. Tectonic and eustatic control on Mishrif regional reservoir distribution. In: Society of Petroleum Engineers Conference in Abu Dhabi, pp. 1–16.
Wells, M., Bowman, A., Kostic, B., Campion, N., Finucane, D., Santos, C., Kitching, D., Brown, R., 2019. Lower Cretaceous deltaic deposits of the main pay reservoir, Zubair Formation, southeast Iraq: depositional controls on reservoir performance. AAPG 16, 219–260.
Zhao, L., Zhou, W., Zhong, Y., Guo, R., Jin, Z., Chen, Y., 2019. Control factors of reservoir oil-bearing difference of Cretaceous Mishrif Formation in the H oilfield, Iraq. Petrol. Explor. Dev. 46 (2), 314–323.